# Minimum Weight Design of Cylindrical Structures

HAROLD SWITZKY* AND JOHN W. CARY†
*Republic Aviation Corporation, Farmingdale, N. Y.*

**A nondimensional design procedure for minimum weight is presented in terms of geometric and material parameters. These are evaluated readily from the type of construction, boundary conditions, and stress-strain data. A nondimensional approach has been employed in order to obtain a simple and rapid design procedure that is applicable to the infinite possible variations of the material and geometrical properties. Each design graph is applicable for all materials and temperatures, thus enabling a designer to evaluate the effects of different materials, temperatures, loads, end fixities, and empirical analysis constants upon the minimum weight design. This technique has been developed in a report[2] to obtain design graphs for columns, unreinforced and reinforced plate, and sandwich construction, which are subjected to compression or shear loads, and for beams in bending. Design graphs and illustrative examples for monocoque and corrugated cylinders subjected to axial compression, torsion, or external radial pressure are presented in this paper.**

A STRUCTURE that can become unstable can be visualized as a set of deformational springs acting in parallel (coupled stability modes) and series (uncoupled stability modes), each of which exhibits instability (radical reduction in stiffness) at respective critical loads. The parallel springs can be viewed as an equivalent spring, with an instability load $P = P_1P_2/(P_1 + P_2)$, in series with the other springs. The critical load of the structure corresponds to the load that causes instability in the weakest (least stable) spring in the series. This critical load can be increased by a redistribution of the area in the structure so as to increase the strength of the weakest spring, usually at the expense of the stronger springs. The optimum distribution of area is that distribution which minimizes the difference between the increased strengths of the weaker springs and the decreased strength of the strongest (most stable) spring. This principle, together with the load equation, can be used to determine the unspecified dimensions of the structure.

It is assumed that a minimum weight design results when the instability in all modes, acting independently, occurs simultaneously. Experience and experimental investigations (e.g., Fig. 1.3 of Ref. 1) indicate that instability in any one mode tends to increase the possibility of failure by decreasing the stiffness and stability in all other modes. If all the modes are made equally stable, then there is no interaction, and the stability of each mode can be defined by an independent stability equation. Attainment of instability in any mode will then result in instability in all modes and a collapse of the structure.

When the number ($n$) of unspecified dimensions is equal to, or less than, the number of possible buckling modes, then the minimum weight design occurs when the stability stresses of the $n$ lowest modes are made equal. If there are more unspecified dimensions than there are possible buckling modes, then additional restrictions must be imposed to obtain the minimum weight design. These additional constraints may be equations defining an optimum stress level or area distribution resulting in a minimum weight.

The general technique is to employ the forementioned defining conditions, together with the load equation, to determine the stress corresponding to the least weight and to solve for the unknown dimensions of the structure knowing this optimum stress.

An example of a structural geometry with one unspecified dimension and one buckling mode is an unreinforced plate. The thickness of the plate is determined from the load equation, which equates the applied load to the product of the failing stress and the area of the cross section (expressible in terms of the stress). If the plate is restrained from buckling, then the maximum allowable stress, e.g., yield, would be optimum.

An example of a structural geometry with two unspecified dimensions and two buckling modes is a tubular column. The load equation and an equation equating the column and local instability stresses are employed. Increasing the diameter ($d$) of a circular tube while maintaining constant cross-sectional area ($\pi dt$) increases the column stability by increasing the inertia but reduces the local (wrinkling) stability by reducing the $t/d$ ratio. The minimum weight design occurs when the stability stresses are made equal. Any other design would result in a reduction of one of the stabilities and a lower efficiency for the structure.

An example of three unknown dimensions is a bent up channel with equal flanges. If the channel is too short to buckle as a column, then the optimum stress is the maximum stress of the material, since only the flange and web buckling modes are possible. If it can only buckle about one axis, then the load equation and the equality of column, flange, and web stability stresses determine the design. If it can buckle about both axes, then the equality of the stability stresses of the column and the least stable element (flange or web) are employed in establishing the design.

A variable-thickness channel with equal flanges possesses four unknown dimensions. If four modes of failure are possible, i.e., buckling about both axes and plate instability of the web and flanges, then, as previously indicated, the load and equal stability criteria generate a minimum weight design. If, however, column buckling can occur only about one axis, then an area distribution that maximizes the instability stress must be employed. This is accomplished by maximizing the appropriate radius of gyration while maintaining the equality of web, flange, and column instability stresses. Similar design techniques can be established for other types of members and loads, e.g., compression, shear, and bending.

Table 1 indicates the proper area distribution for the minimum weight design of a few column cross sections. The area distributions will result in maximum compressive stresses for the instability modes considered. The resulting

Presented at the AIAA Launch and Space Vehicle Shell Structures Conference, Palm Springs, Calif., April 1–3, 1963. This paper is based in part on Aeronautical Systems Division Rept. TDR-62-763, under Contract No. AF33(657)-7872, administered by J. R. Johnson, Project Engineer, Structures Branch, Flight Dynamics Laboratory.

* Head, Configuration Development. Member AIAA.
† Senior Structures Engineer, Structural Development Section.

area and inertia of these cross sections expressed in terms of the dimensions of the least stable element also are presented.

A selection of a type of construction would indicate the known and unknown dimensions, probable modes of failure, and applicable stability equations. The corresponding boundary conditions then suggest the magnitude of the stability constants and expressions for the effective stability modulus. Values of stability constants (or constants from which they can be derived) as well as expressions for the effective stability moduli in terms of the edge fixities and aspect ratios are readily available in the literature, e.g., Refs. 1–9. A summary of such values is found in Refs. 4 and 6.

The solution of the type of equations described previously may be obtained readily if the minimum weight stability

**Table 1 Geometric factors for columns**

| Section | Defining Condition | z | $\alpha_1$ | | $\alpha_3$ | | Thick. Ratio |
|---|---|---|---|---|---|---|---|
| | | wh/dt | A/dt | A/wt | I/d³t | I/w³t | h/t[a] |
| I-Beam | | | 1+4z | 4+1/z | .083+z | 1.333 h/t | |
| | Max $I_{xx}$ | .083 | 1.333 | - | .167 | - | - |
| | $I_{xx}=I_{yy}$ | 2.370<br>.470 | 10.480<br>- | -<br>6.124 | 2.450<br>- | -<br>.667 | -<br>.500 |
| | $I_{xx}=41_{yy}$ | .643<br>.250 | 3.584<br>- | -<br>8.000 | .729<br>- | -<br>.667 | -<br>.500 |
| Channel | | | 1+2z | 2+1/z | .083+.5z | .667-1/(2+1/z) | |
| | Max $I_{xx}$ | .167 | 1.333 | - | .167 | - | - |
| | $I_{xx}=I_{yy}$ | 7.90<br>1.366 | 16.80<br>- | -<br>2.732 | 4.033<br>- | -<br>.301 | -<br>1.000 |
| | $I_{xx}=41_{yy}$ | 1.72<br>.639 | 4.44<br>- | -<br>3.565 | .943<br>- | -<br>.386 | -<br>1.000 |
| Tee | | | 1+2z | 2+1/z | .333-25/(1+2z) | .667 h/t | |
| | Max $I_{xx}$ | .063 | 1.125 | - | .111 | - | - |
| | $I_{xx}=I_{yy}$ | .570<br>.553 | 2.140<br>- | -<br>3.81 | .216<br>- | -<br>.333 | -<br>.500 |
| | $I_{xx}=41_{yy}$ | .250<br>.356 | 1.500<br>- | -<br>4.81 | .167<br>- | -<br>.333 | -<br>.500 |
| Angle[c] | | | 1+z | 1+1/z | .333-25/(1+z) | | |
| | Max $I_{xx}$ | .125 | 1.125 | - | .111 | - | .354 |
| | An angle free to bend about any axis would not buckle about x or y axes. | | | | | | |
| Square Tube | | | 2+2z | | .167+.5z | | |
| | Max $I_{xx}$ | .167 | 2.333 | - | .250 | - | .409 |
| | $I_{xx}=I_{yy}$ | 1.000 | 4.000 | - | .667 | - | 1.000 |
| | $I_{xx}=41_{yy}$ | .090 | 2.180 | - | .212 | - | .300 |
| Circular Tube | - | - | 3.142 | - | .393 | - | - |

(a) Unspecified h/t is defined by $\frac{h}{t} = (z)^{1/2}(C_t/C_h)^{1/4}$
Specified h/t is defined by sheet metal construction or by above equation
(b) X-axis and Y-axis are horizontal and vertical references axes, respectively, for all sections
(c) Angle assumed to bend about x axis only

stress is below the proportional limit. This results in linear equations with direct solutions of the required dimensions. Unfortunately, this situation seldom is satisfied except when the applied loads are very small or when the material is linear up to the maximum allowable stress. In general, the optimum design, especially at high temperatures, occurs at material stresses that are well beyond the proportional limit and requires the solution of nonlinear equations. These equations cannot be solved directly, but a graphical inverse solution can be obtained. Employing a mathematical representation of the stress-strain relationship with three material constants [$E_A\epsilon/\sigma_0 = (1-\beta)\sigma/\sigma_0 + \beta \sinh\sigma/\sigma_0$] and expressing the equations in nondimensional form results in nondimensional design curves applicable to all materials and arbitrary stability constants. The load equation is transformed into an equality between a nondimensional load-geometry-material parameter ($\bar{P}$) and functions of a nondimensional stress ratio ($\sigma/\sigma_0$) and a nondimensional geometry-material parameter ($\xi$). The parameter ($\xi$) is a function of the geometric ratios determining the critical stresses in the various instability modes and is also expressible as a function of the stress ratio [$\xi = (\sigma/\sigma_0)/(E_R/E_A)$].

The derivation of the nondimensional minimum weight design curves is illustrated below for a monocoque cylinder in compression. The load ($P$) in pounds per inch is expressed in terms of the dimensions of the cross section [thickness $h$ (unknown) and radius $R$ (known)] and the stability stress ($\sigma$), that is,

$$P = A\sigma = h\sigma \tag{1}$$

The load equation is modified to obtain a nondimensional form in terms of the stress ratio and any "thickness ratios" that are employed in the stability equations:

$$P/R\sigma_0 = (h/R)(\sigma/\sigma_0) \tag{2}$$

The thickness ratio is converted to an equivalent expression of the geometry-material parameter by manipulation of the stability equation [$\sigma = 9.56\,(E_TE_S)^{1/2}(h/R)^{8/5}$]. This equation is obtained by modifying Eq. (67) [$\sigma = C(E_TE_S)^{1/2}(h/R)$] of Ref. 7 by determining the value of $C = 9.56\,(h/R)^{3/5}$ which matches the experimental data presented in Fig. 7 of the referenced report. Thus,

$$\xi_c^{1/2}\xi_s^{1/2} = \left(\frac{\sigma/\sigma_0}{E_T/E_A}\right)^{1/2}\left(\frac{\sigma/\sigma_0}{E_S/E_A}\right)^{1/2} = \frac{\sigma/\sigma_0}{(E_TE_S)^{1/2}/E_A} = \frac{9.56(E_TE_S)^{1/2}(h/R)^{8/5}}{\sigma_0(E_TE_S)^{1/2}/E_A} = 9.56\frac{E_A}{\sigma_0}\left(\frac{h}{R}\right)^{8/5} \tag{3}$$

and

$$\frac{h}{R} = \left(\frac{\xi_c^{1/2}\xi_s^{1/2}\sigma_0}{9.56\,E_A}\right)^{5/8} = \frac{P}{R\sigma} \tag{4}$$

Substituting Eq. (4) into Eq. (2) and placing the $\sigma/\sigma_0$ and $\xi$ arguments on one side of the equation results in

$$\bar{P} = \frac{P}{R\sigma_0}\left(\frac{9.56\,E_A}{\sigma_0}\right)^{5/8} = \xi_c^{5/16}\xi_s^{5/16}\frac{\sigma}{\sigma_0} \tag{5}$$

where

$\xi_c = (\sigma/\sigma_0)/(E_T/E_A)$; $E_T$ = tangent modulus
$\xi_s = (\sigma/\sigma_0)/(E_S/E_A)$; $E_S$ = secant modulus
$\sigma_0$ = work-hardening parameter
$E_A$ = Young's (initial) modulus

Derivations for the load index ($\bar{P}$) and the unknown dimensions were obtained for monocoque and corrugated cylinders of moderate length which were subjected to compression, radial pressure, or torsion loads. The design curves are presented in Figs. 1–9. The equations and curves are based upon the stability equations obtained from Refs. 7 and 9. Future experience or analysis can be adapted to the design procedure. Empirical constants can be incorporated in the same design graphs, but changes in the exponents of the "thickness ratios" may require new design graphs.

The usual design problem for monocoque cylinders may be formulated as follows. Given radius ($R$), length ($L$), and loading, find optimum skin thickness ($h$). For the cylinder under uniform radial pressure ($p$), one finds [using Eq. (55) of Ref. 7 and the pressure buckling coefficient for moderate

length cylinders of Ref. 9, reduced to the isotropic case]

$$\bar{P} = \left\{\frac{0.901}{(1-\nu^2)^{1/2}}\right\}\left(\frac{p}{\sigma_0}\right)\left(\frac{E_A}{\sigma_0}\right)^{2/3}\left(\frac{R}{L}\right)^{2/3} = C_1\left(\frac{p}{\sigma_0}\right)\left(\frac{E_A}{\sigma_0}\right)^{2/3}\left(\frac{R}{L}\right)^{2/3} = \xi_p{}^{2/3}\left(\frac{\sigma}{\sigma_0}\right) \quad (6)$$

$$h = \frac{1}{C_1}\left(\frac{\xi_p\sigma_0}{E_A}\right)^{2/3} L^{2/3}R^{1/3} = \frac{pR}{\sigma} \quad (7)$$

where

$\xi_p = (\sigma/\sigma_0)/(E_R/E_A)$

$E_R = E_S\{0.428 + 0.572[0.25 + 0.75(E_T/E_S)]^{1/2}\}$

= average value of effective modulus for various boundary conditions

For a cylinder loaded by a torque ($T$), one finds [using the suggested experimentally determined modifications of Eq. (A7) of Ref. 7]

$$\bar{P} = \left\{\frac{0.757}{(1-\nu^2)^{1/2}}\right\}\left(\frac{T}{R^3\sigma_0}\right)\left(\frac{R}{L}\right)^{2/5}\left(\frac{E_A}{\sigma_0}\right)^{4/5} = \xi_s{}^{4/5}\left(\frac{\tau 3^{1/2}}{\sigma_0}\right) \quad (8)$$

$$h = 1.53\,(1-\nu^2)^{1/2}\left(\frac{\sigma_0\xi_s}{E_A}\right)^{4/5} L^{2/5}R^{3/5} = \frac{T}{2\pi R^2\tau} \quad (9)$$

The following design equations use the general stability equations for moderate-length orthotropic cylinders as presented in Ref. 9. These stability analyses are based upon the following assumptions and conditions: 1) linear small-deflection theory is applicable; 2) the connections between the outer skins and the stiffening elements are monolithic; 3) Poisson's ratio ($\nu$) = 0; and 4) the skin is isotropic.

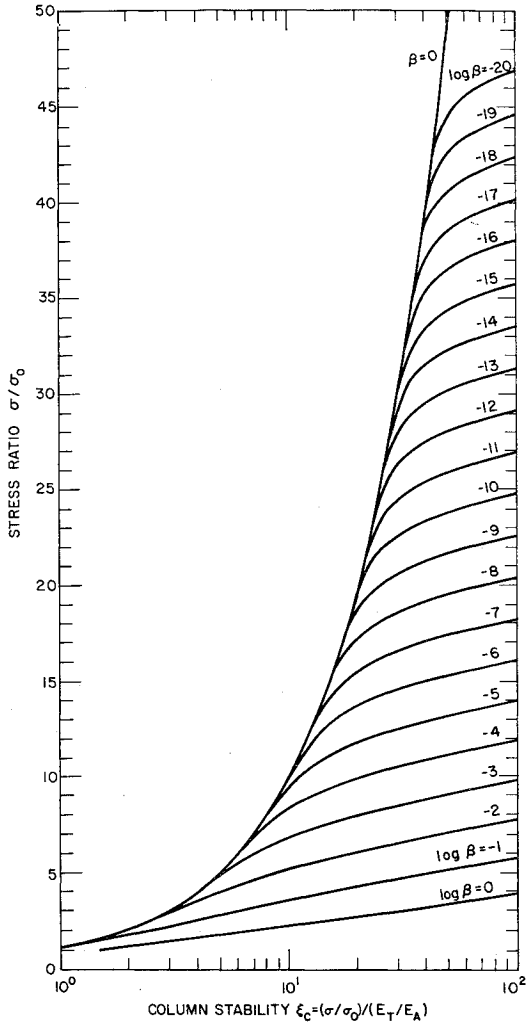


**Fig. 1 Stress ratio vs column stability parameter.**

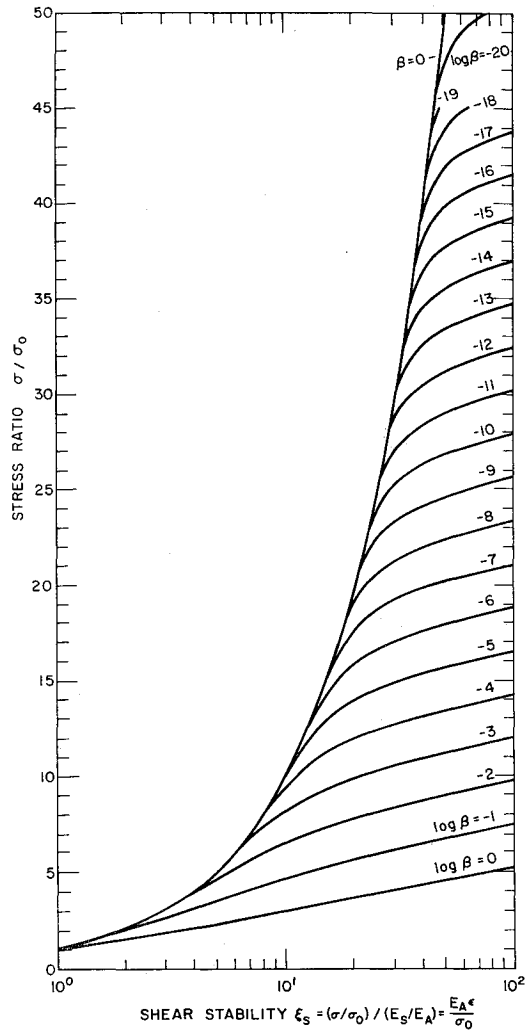


**Fig. 2 Nondimensional stress-strain curves.**

For simplicity, only one type of stiffener system is treated in this paper, namely, corrugated skin stiffening of the type shown in Fig. 10. In the case of axial compression, the corrugations are taken parallel to the longitudinal axis, whereas in the case of torsion and radial pressure, the corrugations are in the circumferential direction.

The common design problem for corrugated orthotropic cylinders can be formulated as follows. Given radius ($R$), length ($L$), flats ratio ($n$), corrugation angle ($\theta$), and loading, find the optimum characteristic dimensions of the corrugation, i.e., web thickness ($t$) and height ($d$), and the optimum skin thickness ($h'$).

For the single-face corrugated cylinder under uniform radial pressure ($p$), use is made of Eqs. (4) and (17) of Ref. 9 which contain the assumption that the circumferential wavelength is much shorter than the axial wavelength. The design equations are

$$\bar{P} = \left\{3.12\left(\frac{\alpha_4{}^{1/2}\alpha_6{}^{1/6}}{\alpha_1{}^{5/3}}\right) C_t{}^{1/2}\sin\theta\right\}\left(\frac{p}{\sigma_0}\right)\left(\frac{E_A}{\sigma_0}\right)^{7/6}\left(\frac{R}{L}\right)^{2/3}$$

$$= C_3\left(\frac{p}{\sigma_0}\right)\left(\frac{E_A}{\sigma_0}\right)^{7/6}\left(\frac{R}{L}\right)^{2/3} = \xi_p{}^{7/6}\left(\frac{\sigma}{\sigma_0}\right) \quad (10)$$

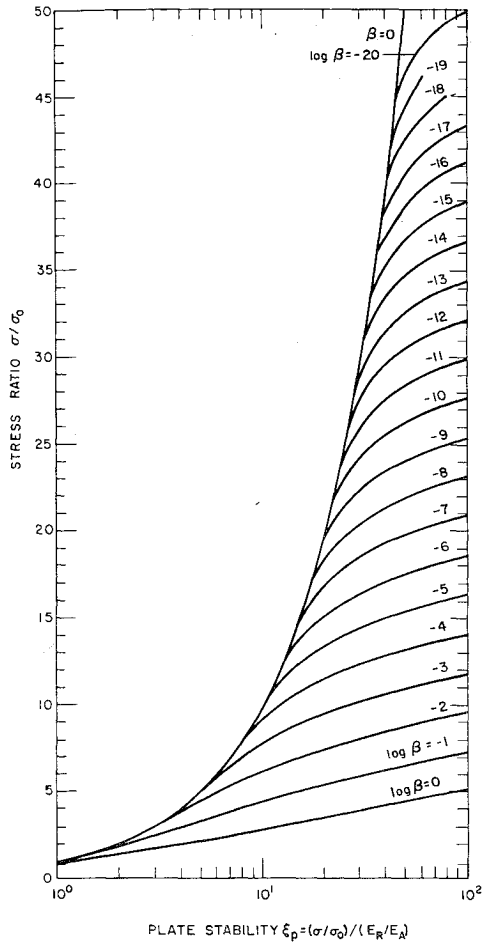


**Fig. 3 Stress ratio vs plate stability parameter.**

$$t = (LR^{1/2})^{2/3}\left(\frac{1}{\alpha_1 C_3}\right)\left(\frac{\xi_p\sigma_0}{E_A}\right)^{7/6} = \frac{pR}{\alpha_1\sigma} \tag{11a}$$

$$d = t(C_t E_A/\xi_p\sigma_0)^{1/2}\sin\theta \tag{11b}$$

$$h = \alpha_6 t \tag{11c}$$

where

$$\alpha_6 = 2(n\sin\theta + \cos\theta)(C_t/C_h)^{1/2}$$

= ratio of skin thickness to corrugation web thickness (12a)

$$\alpha_1 = \frac{n\sin\theta + 1}{n\sin\theta + \cos\theta} + 2\left(\frac{C_t}{C_h}\right)^{1/2}(n\sin\theta + \cos\theta)$$

= ratio of average corrugation area per inch to corrugation web thickness (12b)

$$\alpha_4 = \frac{I_{xx}}{d^2 t} = \frac{(n/4)\sin\theta + \frac{1}{12}}{n\sin\theta + \cos\theta} + \frac{\frac{1}{2}(C_t/C_h)^{1/2}(n\sin\theta + 1)}{\alpha_1} \tag{12c}$$

where $C_t$ and $C_h$ (stability coefficients for the web and skin in compression) are 3.62 for simple supports.

Equations (4) and (21) of Ref. 9 are employed for the single-faced corrugated cylinder loaded by a torque ($T$). The equations contain the assumption that the axial buckle wavelength is much shorter than the circumferential wavelength. The design equations are

$$\bar{P} = \left\{\frac{0.740 S_t^{1/2}\alpha_9^{1/2}\alpha_7^{4/5}\sin\theta}{\alpha_8^{9/5}}\right\}\left(\frac{T}{\sigma_0 R^3}\right)\left(\frac{R}{L}\right)^{2/5}\left(\frac{3^{1/2}E_A}{\sigma_0}\right)^{13/10}$$

$$= C_4\left(\frac{T}{\sigma_0 R^3}\right)\left(\frac{R}{L}\right)^{2/5}\left(\frac{3^{1/2}E_A}{\sigma_0}\right)^{13/10} = \xi_s^{13/10}\left(\frac{\tau 3^{1/2}}{\sigma_0}\right) \tag{13}$$

$$t = (L^{1/2}R^{3/4})^{4/5}\left(\frac{3^{1/2}}{2\pi\alpha_8 C_4}\right)\left(\frac{\xi_s\sigma_0}{E_A 3^{1/2}}\right)^{13/10} = \frac{T}{2\pi R^2\alpha_8\tau} \tag{14a}$$

$$d = t\left(\frac{S_t\, 3^{1/2}E_A}{\xi_s\sigma_0}\right)^{1/2}\sin\theta \tag{14b}$$

$$h' = \alpha_7 t \tag{14c}$$

where $S_t$ and $S_h$ (4.82 for simple supports) are stability coefficients for the corrugation web and skin elements in shear, and where

$$\alpha_7 = 2[(S_t/S_h)^{1/2}(n\sin\theta + 1)(n\sin\theta + \cos\theta)]^{1/2} \tag{15a}$$

= ratio of skin thickness to corrugation web thickness

$$\alpha_8 = \left[\left(\frac{n\sin\theta + 1)}{n\sin\theta + \cos\theta}\right)\alpha_7 + 1\right] \tag{15b}$$

= ratio of effective shear area per inch to corrugation web thickness

$$\alpha_9 = \frac{I_{xx}}{d^2 t} = \frac{(n/4)\sin\theta + \frac{1}{12}}{n\sin\theta + \cos\theta} + \frac{\alpha_7}{4}\left[\frac{n\sin\theta + 1}{n(\alpha_7 + 1)\sin\theta + 1 + \alpha_7\cos\theta}\right] \tag{15c}$$

Because of the relatively poor agreement between experimental data and orthotropic theory as applied to reinforced cylinders in compression, an alternate approach seems indicated. The technique employed in this paper is to analyze a double-faced corrugated cylinder as an "equivalent" isotropic cylinder having a cross-sectional radius of gyration ($h_e/12^{1/2}$) equal to that of the corrugated cylinder. The bending stiffness of the corrugated cylinder was approximated by employing orthotropic flat plate theory [Eq. (233) of Ref. 3]. In order to obtain the design equations and curves for the corrugated cylinder in compression, the semi-empirical stability equation [$\sigma = 9.56(E_T E_S)^{1/2}(h_e/R)^{1.6}$] was used with the restriction that the stability stress would not exceed the classical solution for a perfect isotropic cylinder [$\sigma = 0.6(E_T E_S)^{1/2}(h_e/R)$, i.e., $h_e/R \leq 0.0098$]. This results in

$$\bar{P} = \left\{\frac{10.03 C_t^{1/2}}{(\sin\theta)^{5/4}}\left[\frac{(\alpha_{42}\alpha_{52})^{1/2} + \alpha_{52}}{\alpha_{12}^3}\right]^{1/2}\right\}\left(\frac{P}{\sigma_0 R}\right)\left(\frac{E_A}{\sigma_0}\right)^{9/8}$$

$$= C_5\left(\frac{P}{\sigma_0 R}\right)\left(\frac{E_A}{\sigma_0}\right)^{9/8} = \xi_p^{9/8}\frac{\sigma}{\sigma_0} \tag{16}$$

**Fig. 4 Stress ratio vs load index for a monocoque cylinder in axial compression.**

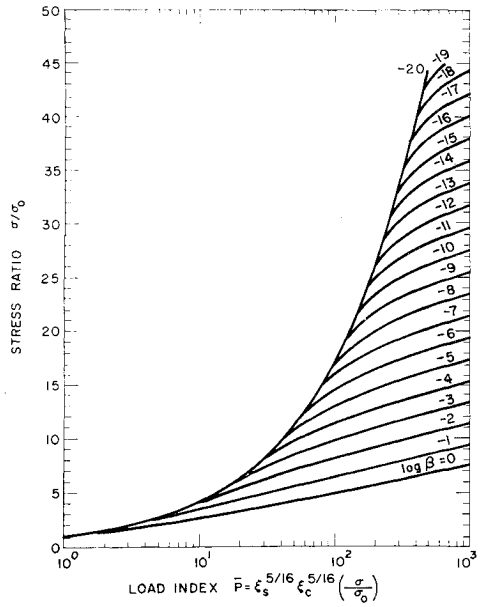

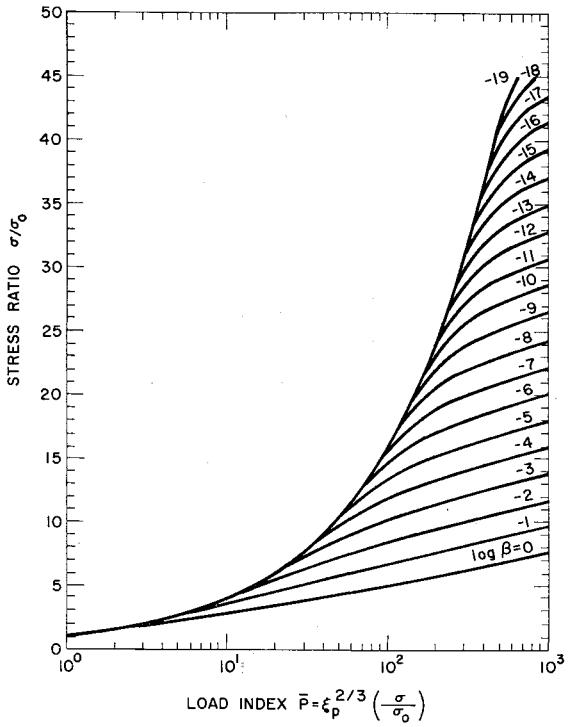


**Fig. 5 Stress ratio vs load index for a monocoque cylinder under external radial pressure.**

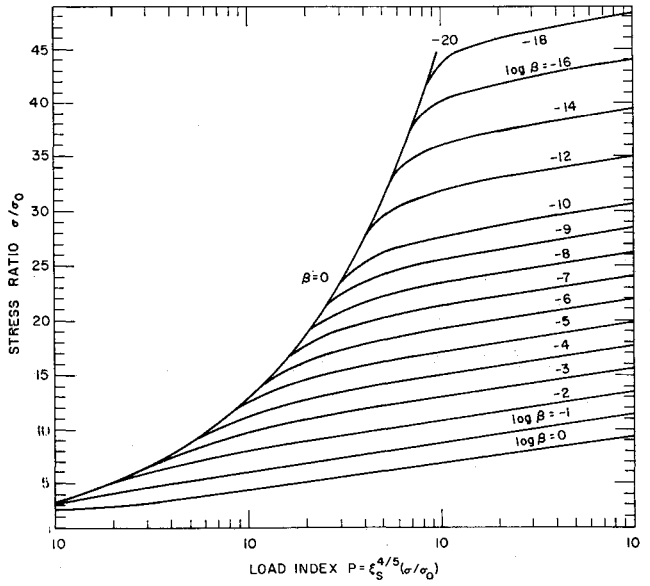


**Fig. 6 Stress ratio vs load index for a monocoque cylinder in torsion.**

$$d = \left(\frac{C_t^{1/2}}{C_s\alpha_{12}(\sin\theta)^{5/4}}\right)\left(\frac{\xi_p\sigma_0}{E_A}\right)^{5/8}R \tag{17a}$$

$$t = \frac{d}{\sin\theta}\left(\frac{\xi_p\sigma_0}{C_tE_A}\right)^{1/2} = \frac{PR}{\alpha_{12}\sigma} \tag{17b}$$

$$h' = \alpha_6 t \tag{17c}$$

where

$$\alpha_{12} = \frac{n\sin\theta + 1}{n\sin\theta + \cos\theta} + 4\left(\frac{C_t}{C_h}\right)^{1/2}(n\sin\theta + \cos\theta) \tag{18a}$$

ratio of area per inch to corrugation web thickness is

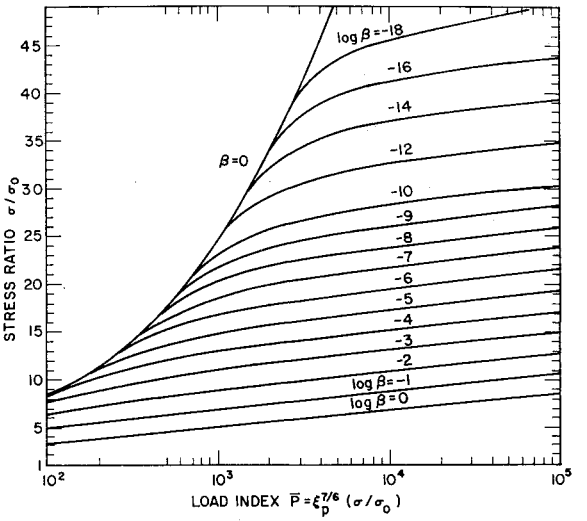


**Fig. 7 Stress ratio vs load index for a single-faced corrugated cylinder under uniform external radial pressure.**

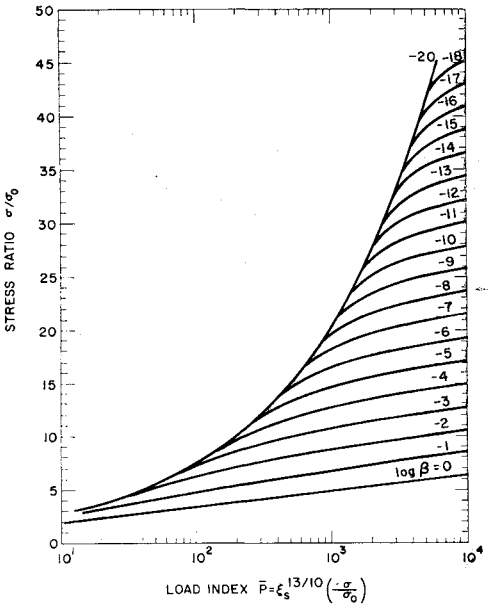


**Fig. 8 Stress ratio vs load index for single-faced corrugated cylinder in torsion.**

$$\alpha_{52} = I_{yy}/td^2 = (C_t/C_h)^{1/2}(n\sin\theta + \cos\theta) \tag{18c}$$

Equations (12, 15, and 18) for the geometric ratios ($\alpha$) are derived in Ref. 2 from equations of equal stability and compatibility.

The minimum weight design is obtained by first evaluating $\bar{P}$ from the known applied load, geometry, and structural material, then determining the optimum stress ratio from the applicable $\bar{P}$ vs ($\sigma/\sigma_0$) plot (Figs. 4–9), and finally calculating the design details from the appropriate $\xi$ (Figs. 1–3). The use of nondimensional design curves results in a relatively simple and rapid method of designing a minimum weight structure and significantly reduces the amount of design data and procedures required. The effects of assuming different end fixities, introducing empirical data, and considering different materials or thermal exposures can be evaluated readily by using the same design graphs.

The utility of the nondimensional technique in the inelastic range is dependent upon a satisfactory description

$$\alpha_{42} = \frac{I_{xx}}{td^2} = \frac{(n/4)\sin\theta + \frac{1}{12}}{n\sin\theta + \cos\theta} + \left(\frac{C_t}{C_h}\right)^{1/2}(n\sin\theta + \cos\theta) \tag{18b}$$

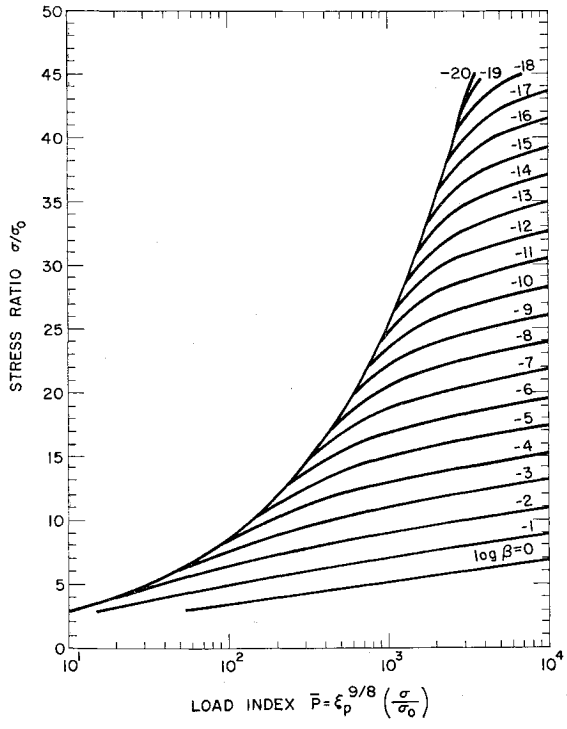


**Fig. 9 Stress ratio vs load index for a double-faced corrugated cylinder in axial compression.**

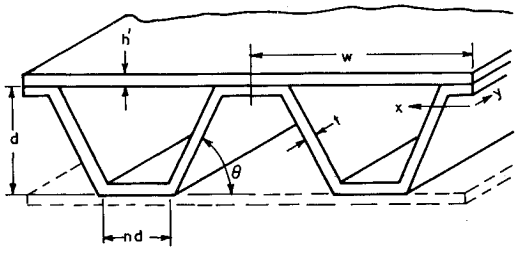


**Fig. 10 Corrugation details.**

of the stress-strain relationship. The following formulation, based upon a rate diffusion model of deformations (representing the nonlinear strain as an exponential function of the stress) is employed:

$$\frac{E_A\epsilon}{\sigma_0} = \frac{\sigma}{\sigma_0}(1-\beta) + \beta \sinh\frac{\sigma}{\sigma_0} = \xi_s \qquad (19)$$

This formulation is in good agreement with experimental data and has been employed to approximate isochronous as well as instantaneous stress-strain curves. Stress-strain curves in shear are obtained by assuming an invariant octohedral stress-strain law that results in the following transformations:

$$\tau = \sigma/3^{1/2} \qquad (20a)$$

and

$$\gamma = 2(1+\nu)\epsilon/3^{1/2} \qquad (20b)$$

The formulation [Eq. (19)] is readily adaptable to a computer program to plot the desired nondimensional design curves. It offers the widest latitude in matching the actual stress-strain curve while still resulting in a single design graph for a given type of construction.

The material constants are chosen to match the initial portion of the stress-strain curve up to the area of interest in the design. This requires matching the linear and nonlinear portions of the curve up to the vicinity of the yield stress. Selecting $E_A$ equal to the initial slope of the curve

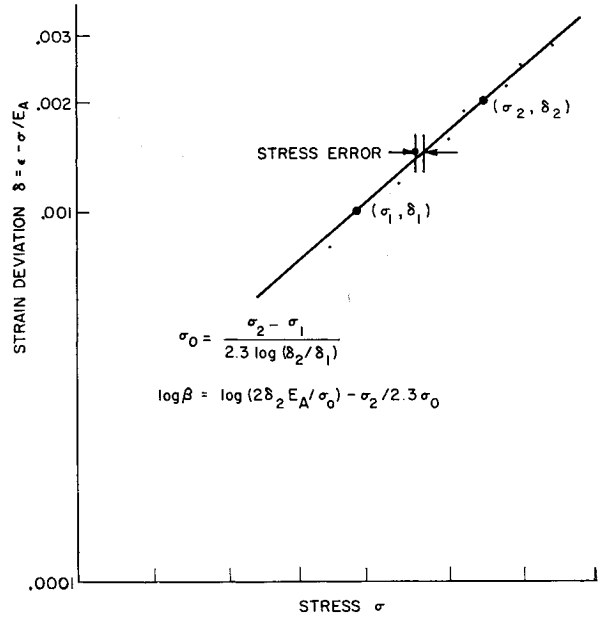


**Fig. 11 Strain deviation vs stress.**

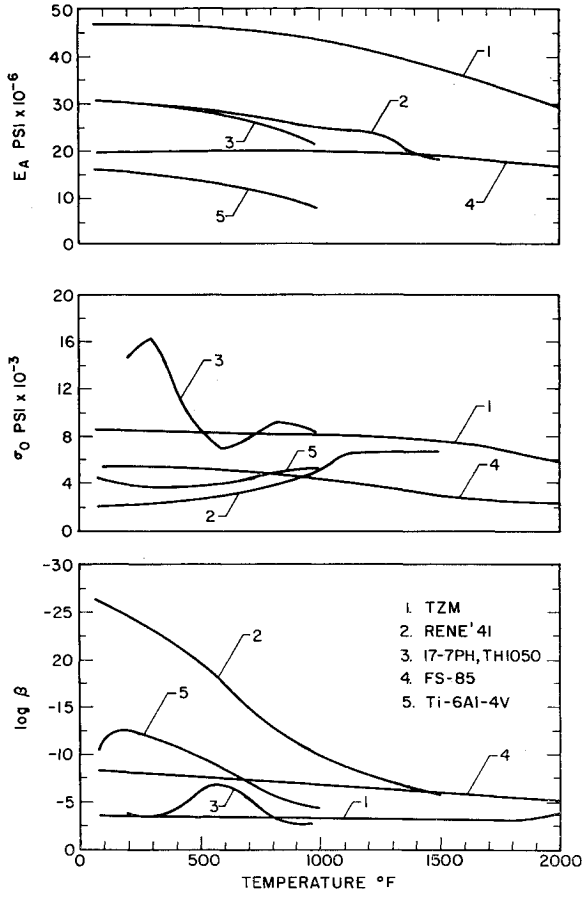


**Fig. 12 Material constants $E_A$, $\sigma_0$, and log$\beta$ vs temperature.**

matches the initial portion of the curve. The remaining constants $\sigma_0$ (the work-hardening parameter) and $\beta$ (the nonlinear parameter) are selected to match the nonlinear portion of the curve. One procedure is to plot the strain deviation ($\delta = \epsilon - \sigma/E_A$) on a log scale vs values of the stress ($\sigma$) on a linear scale (Fig. 11). This plot results in a straight line for the plastic portion of the stress-strain curve if the formulation is absolutely correct. Selecting values of $\sigma_0$ and $\beta$ which depend upon the best straight line results in a good approximation to the actual curve with the error

**Table 2a Radial pressure loading**

| Item | Reference | Radial pressure 15 psi | Radial pressure 600 psi |
|---|---|---|---|
| Monocoque cylinder | | | |
| $\bar{P} = 0.945\left(\frac{p}{\sigma_0}\right) \times \left(\frac{E_A}{\sigma_0}\right)^{2/3}\left(\frac{R}{L}\right)^{2/3}$ | Eq. (6) | 0.287 | 11.48 |
| $\frac{\sigma}{\sigma_0}$ | Fig. 5 | 0.473 | 4.33 |
| $\sigma = \left(\frac{\sigma}{\sigma_0}\right) 5000$ | | 2365 psi | 21,650 psi |
| $h = \frac{PR}{\sigma}$ | Eq. (7) | 0.634 in. | 2.77 in. |
| Corrugated cylinder ($\alpha_1 = 4$; $\alpha_4 = \frac{7}{12}$; $\alpha_6 = 2$) | | | |
| $\bar{P} = 0.505\left(\frac{P}{\sigma_0}\right) \times \left(\frac{E_A}{\sigma_0}\right)^{7/6}\left(\frac{R}{L}\right)^{2/3}$ | Eq. (10) | 7.11 | 284 |
| $\frac{\sigma}{\sigma_0}$ | Fig. 7 | 2.47 | 12.6[a] |
| $\sigma = \left(\frac{\sigma}{\sigma_0}\right) 5000$ | | 12,350 psi | 63,000 psi |
| $\xi_p$ | Fig. 3 | 2.47 | 15.0 |
| $t = \frac{pR}{\alpha_1\sigma}$ | Eq. (11a) | 0.030 in. | 0.238 in. |
| $d = t\left(\frac{C_t E_A}{\xi_p \sigma_0}\right)^{1/2}$ | Eq. (11b) | 1.66 in. | 5.28 in. |
| $h' = \alpha_6 t$ | Eq. (11c) | 0.061 in. | 0.476 in. |
| $\bar{W} = h/\alpha_1 t$ | | 5.2 | 2.9 |

[a] Stress beyond apparent proportional limit ($\sigma/\sigma_0 \sim 10.6$).

**Table 2b Torsion loading**

| Item | Reference | Torque $5 \times 10^7$ in. lb | Torque $10^9$ in. lb |
|---|---|---|---|
| Monocoque cylinder | | | |
| $\bar{P} = 0.793\left(\frac{T}{R^3\sigma_0}\right) \times \left(\frac{R}{L}\right)^{2/5}\left(\frac{E_A}{\sigma_0}\right)^{4/5}$ | Eq. (8) | 2.71 | 54.1 |
| $\frac{\sigma}{\sigma_0}$ | Fig. 6 | 1.738 | 9.18 |
| $\tau = \frac{1}{3^{1/2}}\left(\frac{\sigma}{\sigma_0}\right) 5000$ | | 5,010 psi | 26,480 psi |
| $h = \frac{T}{2\pi R^2 \tau}$ | Eq. (9) | 0.159 in. | 0.601 in. |
| Corrugated cylinder ($\alpha_1 = 4.828$; $\alpha_9 = 0.627$; $\alpha_7 = 2.828$; $\alpha_8 = 6.656$) | | | |
| $\bar{P} = 0.098\left(\frac{T}{R^3\sigma_0}\right) \times \left(\frac{R}{L}\right)^{2/5}\left(\frac{3^{1/2}E_A}{\sigma_0}\right)^{13/10}$ | Eq. (13) | 30.6 | 612 |
| $\frac{\sigma}{\sigma_0}$ | Fig. 8 | 4.43 | 14.7[a] |
| $\tau = \frac{1}{3^{1/2}}\left(\frac{\sigma}{\sigma_0}\right) 5000$ | | 12,800 psi | 42,200 psi |
| $\xi_s$ | Fig. 2 | 4.43 | 19 |
| $t = \frac{T}{2\pi R^2 \alpha_1 \tau}$ | Eq. (14a) | 0.0129 in. | 0.078 in. |
| $d = t\left(\frac{S_t 3^{1/2} E_A}{\xi_s \sigma_0}\right)^{1/2}$ | Eq. (14b) | 0.675 in. | 2.33 in. |
| $h' = \alpha_7 t$ | Eq. (14c) | 0.036 in. | 0.219 in. |
| $\bar{W} = h/\alpha_1 t$ | | 2.6 | 1.6 |

[a] Stress beyond apparent proportional limit ($\sigma/\sigma_0 \sim 10.6$).

in the stress represented by the horizontal distance between an actual point and the straight line in the referenced plot. The material constants $\sigma_0$ and $\beta$ are determined [after two points ($\sigma_1$, $\delta_1$) and ($\sigma_2$, $\delta_2$) on the best straight line are selected] by the following equations:

$$\sigma_0 = \frac{\sigma_2 - \sigma_1}{2.3 \log(\delta_2/\delta_1)} \tag{21a}$$

and

$$\log\beta = \log\left(\frac{E_A}{\sigma_2 - \sigma_1}\right) + \log\left(4.6\delta_2 \log\frac{\delta_2}{\delta_1}\right) - \frac{[\log(\delta_2/\delta_1)]\sigma_2}{\sigma_2 - \sigma_1} \tag{22a}$$

Requiring the approximation of the stress-strain curve to pass through two nonlinear points on the actual curve is equivalent to selecting the stress and deviation of these two points in order to establish the straight line. As an example, if the 0.001 and 0.002 offset stresses are employed, then

$$\sigma_0 = 1.442(\sigma_2 - \sigma_1) \tag{21b}$$

and

$$\log\beta = \log\left(\frac{E_A}{\sigma_2 - \sigma_1}\right) - 2.558 - \left[\frac{0.301\sigma_2}{\sigma_2 - \sigma_1}\right] \tag{22b}$$

The resulting computed stress-strain curve [Eq. (19)] will match the yield stress ($\sigma_2$), the 0.001 offset stress ($\sigma_1$), and have an initial modulus equal to $E_A$. If the 0.0002 offset stress ($\sigma_1$ = proportional limit) and yield stress are used, then

$$\sigma_0 = 0.434(\sigma_2 - \sigma_1) \tag{21c}$$

and

$$\log\beta = \log\frac{E_A}{\sigma_2 - \sigma_1} - 3.036 - \frac{\sigma_2}{\sigma_2 - \sigma_1} \tag{22c}$$

Values of the material constants ($E_A$, $\sigma_0$, $\beta$) as a function of temperature are presented for various materials in Fig. 12 to illustrate the type of desirable design data. Scatter in the material constants is to be expected, especially at high temperatures, because of variations in the stress-strain curves. A statistical analysis of all available data is recommended in order to obtain the most probable values of the material constants and to estimate the effect of the variations on the design. Fortunately, the minimum weight is usually not too sensitive to the variations in $\sigma_0$ and $\beta$.

The design examples (Tables 2a–2c) illustrate the proposed design procedure. Both monocoque and corrugated cylinders are designed for particular values of radial pressure, torsion, or axial compression loadings. Two load intensities are considered for each type of loading in order to demonstrate the effect of the load intensity upon the design. The optimum design stresses corresponding to the lower load index are below the proportional limit of the material. For the higher load index, however, the corrugated cylinders have optimum stress levels in the plastic range, whereas the monocoque cylinders remain in the elastic range. The two structural geometries considered are compared on the basis of minimum weight for each loading. The comparison is shown in terms of a weight ratio ($\bar{W}$), where

$$\bar{W} = \frac{\text{monocoque cylinder minimum weight}}{\text{corrugated cylinder minimum weight}}$$

**Table 2c Axial compression loading**

| Item | Reference | Axial load 1500 lb/in. | Axial load 8000 lb/in. |
|---|---|---|---|
| Monocoque cylinder | | | |
| $\bar{P} = \frac{P}{\sigma_0 R}\left(\frac{9.56E_A}{\sigma_0}\right)^{5/8}$ | Eq. (5) | 1.44 | 7.68 |
| $\frac{\sigma}{\sigma_0}$ | Fig. 4 | 1.25 | 3.51 |
| $\sigma = \left(\frac{\sigma}{\sigma_0}\right) 5000$ | | 6260 psi | 17,540 psi |
| $h = \frac{P}{\sigma}$ | Eq. (4) | 0.240 in. | 0.456 in. |
| Corrugated cylinder ($\alpha_{12} = 6$; $\alpha_{42} = \frac{4}{3}$; $\alpha_{52} = 1$) | | | |
| $\bar{P} = 1.91\left(\frac{P}{\sigma_0 R}\right)\left(\frac{E_A}{\sigma_0}\right)^{9/8}$ | Eq. (16) | 30.2 | 161 |
| $\frac{\sigma}{\sigma_0}$ | Fig. 9 | 4.98 | 10.7[a] |
| $\sigma = \left(\frac{\sigma}{\sigma_0}\right) 5000$ | | 24,900 psi | 53,500 psi |
| $\xi_p$ | Fig. 3 | 4.98 | 11.2 |
| $d = R\left(\frac{\xi_p \sigma_0}{E_A}\right)^{5/8}\left(\frac{C_t^{1/2}}{\alpha_{12} C_5}\right)$ | Eq. (17a) | 0.390 in. | 0.650 in. |
| $t = \frac{pR}{\alpha_{12}\sigma}$ | Eq. (17b) | 0.010 in. | 0.025 in. |
| $h' = \alpha_6 t$ | Eq. (17c) | 0.020 in. | 0.050 in. |
| $\bar{W} = h/\alpha_{12} t$ | | 4.0 | 3.1 |

[a] Stress beyond apparent proportional limit ($\sigma/\sigma_0 \sim 10.6$)

When the optimum stress is within the linear range of the material, then a more accurate value for the optimum stress ratio ($\sigma/\sigma_0$) can be obtained directly from the load index ($\bar{P}$) rather than from the design graphs. This is because $\xi_p = \xi_c = \xi_s = \sigma/\sigma_0$ in this range [e.g., if $\bar{P} = \xi_p^{2/3}(\sigma/\sigma_0) = (\sigma/\sigma_0)^{5/3}$, then $(\sigma/\sigma_0) = \bar{P}^{3/5}$].

For the sake of simplifying the presentation of the design technique, a square-wave corrugation is employed ($n = 1$ and $\theta = 90°$) in the stiffened cylinders, all cylinders are designed for a radius of 100 in. and a length of 200 in., and a single material-temperature combination ($T_i$-6Al-4V at 800°F) is considered. The appropriate material constants for this combination (from Fig. 12) are $E_A = 10.2 \times 10^6$ psi, $\sigma_0 = 5000$ psi, and $\log\beta = -5.6$.

The corrugated cylinders are chosen as the design configuration, because prior investigations[2] have shown that the most general optimum design of a plate or cylinder reinforced integrally or by attached stiffeners leads to impractically small stiffener spacings. Practical design restrictions, e.g., fixed stiffener spacing, result in "optimum" designs heavier than the lightest design obtainable. The use of a corrugated skin stiffener system is a good compromise. This system possesses a continuity of stiffener material and has the effect of very close stiffener spacing, although it may not have the area distribution that will cause a node at the stiffener.

One of the desirable features of the proposed design procedure is the ease with which optimum weights for various structural geometries and loadings can be evaluated and compared. The weight comparisons of the illustrative examples indicate that the corrugation-reinforced cylinder is more efficient (lighter) than the monocoque cylinder for all loadings considered. This efficiency advantage is also shown to decrease with increasing load. At sufficiently high load indices, the monocoque geometry will exhibit equal or greater efficiency than the corrugated cylinder. This is because of the convergence of the optimum stresses and the equal or greater effectivity of the monocoque cross section. Similar comparisons involving other geometries or materials can be readily made, thus affording a rapid and convenient method of choosing the best structural geometry-material combination for a given design problem. Any refinement in the stability analysis can be incorporated easily in the design procedure.

## References


[1] Gerard, G., *Minimum Weight Analysis of Compression Structures* (New York University Press, New York, 1956), Chap. 1.

[2] Switzky, H., "The minimum weight design of structures operating in an aerospace environment," Aeronaut. Systems Div. TR-62-763 (October 1962).

[3] Timoshenko, S., *Theory of Elastic Stability* (McGraw-Hill Book Co. Inc., New York, 1936), Chap. VII.

[4] Bleich, F., *Buckling Strength of Metal Structures* (McGraw-Hill Book Co. Inc., New York, 1952), Chaps. IX–XI.

[5] Stowell, E. Z., "A unified theory of plastic buckling of columns and plates," NACA Rept. 898 (1948).

[6] Gerard, G. and Becker, H., "Buckling of flat plates," NACA TN 3781 (July 1957).

[7] Gerard, G. and Becker, H., "Buckling of curved plates and shells," NACA TN 3783 (August 1957).

[8] Shanley, F. R., *Weight-Strength Analysis of Aircraft Structures* (McGraw-Hill Book Co. Inc., New York, 1952), Part 1.

[9] Becker, H. and Gerard, G., "Elastic stability of orthotropic shells," J. Aerospace Sci. 29, 505–512, 520 (1962).